JACS
JOURNAL OF THE AMERICAN CHEMICAL SOCIETY
Communication
pubs.acs.org/JACS

Dip-Pen Nanolithography-Assisted Protein Crystallization

Francesco S. Ielasi,[†] Michael Hirtz,*[,‡] Sylwia Sekula-Neuner,[‡] Thomas Laue,[‡] Harald Fuchs,[§,‡] and Ronnie G. Willaert*[,†]

[†]Department of Bioengineering Sciences, Vrije Universiteit Brussel, 1050 Brussels, Belgium
[‡]Institute of Nanotechnology and Karlsruhe Nano Micro Facility, Karlsruhe Institute of Technology, 76021 Karlsruhe, Germany
[§]Physical Institute and Center for Nanotechnology, Westfälische Wilhelms-Universität, 48149 Münster, Germany

Supporting Information

ABSTRACT: We demonstrate the use of dip-pen nanolithography (DPN) to crystallize proteins on surface-localized functionalized lipid layer arrays. DOPC lipid layers, containing small amounts of biotin-DOPE lipid molecules, were printed on glass substrates and evaluated in vapor diffusion and batch crystallization screening setups, where streptavidin was used as a model protein for crystallization. Independently of the crystallization system used and the geometry of the lipid layers, nucleation of streptavidin crystals occurred specifically on the DPN-printed biotinylated structures. Protein crystallization on lipid array patches is also demonstrated in a microfluidic chip, which opens the way toward high-throughput screening to find suitable nucleation and crystal growth conditions. The results demonstrate the use of DPN in directing and inducing protein crystallization on specific surface locations.

Despite recent advances in experimental biophysical techniques, such as nuclear magnetic resonance (NMR), small-angle X-ray scattering (SAXS), and single-particle cryo-electron microscopy (cryo-EM), X-ray crystallography remains the most widely used method for protein structure determination. This method requires adequately sized three-dimensional (3D) protein crystals of low defect density and high compositional uniformity to obtain high-resolution diffraction data.[1] Frequently, obtaining crystals remains an obstacle to solving their structures.[1,2] Alternatively, the atomic structure of membrane proteins in their native membranous environment can be determined using cryo-EM-based electron crystallography on two-dimensional crystals, which are also not easy to obtain.[3]

As a model for protein crystallization, we selected streptavidin, which finds wide use in molecular biotechnology due to its extraordinary strong affinity for biotin and its ability to self-assemble as two-dimensional (2D) crystals onto biotinylated lipid surfaces under favorable conditions.[4] Among the various lipids that have been used to obtain 2D crystals, 1,2-dioleoyl-*sn*-glycero-3-phosphocholine (DOPC) together with biotinylated lipids such as 1,2-dioleoyl-*sn*-glycero-3-phosphoethanolamine-*N*-(cap biotinyl) (biotin-DOPE) are particularly suitable due to the remarkable fluidity of planar bilayers at room temperature and their low phase-transition temperature, which facilitates the lateral diffusion of bound streptavidin and its subsequent 2D crystallization.[5] A mixture of these lipids was selected for DPN-writing the lipid layer patches. The epitaxial growth of 3D crystals from 2D crystals onto lipid layers have been demonstrated previously for streptavidin,[4c,6] RNA polymerase II,[6a] and lysozyme.[7]

We used DPN to create microarrays of functionalized lipid patches to assist protein crystallization. DPN is a scanning probe-based nanofabrication tool which allows soft-matter surface patterning by taking advantage of the high resolution of the atomic force microscopy (AFM) technique.[8] Several ink substrates can be "printed" by DPN, including small organic molecules, organic polymers, metal salts, and also biological polymers (such as proteins, lipids, and DNA). The parallel printing of surface patterns with one or more ink substrates characterized by different chemical functionalities is also possible with DPN by using linear or 2D arrays of AFM cantilevers.[8a,9] Non-covalent parallel patterning of DOPC fluorescently labeled lipids mixtures on hydrophobic and hydrophilic surfaces by DPN has been performed previously (L-DPN).[10] Furthermore, the L-DPN deposition of supported DOPC membrane nanostructures containing biotin- and/or nitriloacetic-capped lipids has been shown to be a successful strategy for the selective deposition of native or recombinant tagged proteins on glass[11] or graphene.[12] Applications of L-DPN for the production of biomimetic patterns to be used as cell culture substrates[11,13] or for functionalization in biosensing and biocatalysis[12,14] have been demonstrated. The utilization of DPN as a crystallization tool has been demonstrated for small organic molecules, i.e., pentaerythritol tetranitrate (PETN)[15] and organic polymers, i.e., poly-DL-lysine.[16] However, DPN has not yet been used to assist protein crystallization.

Here we demonstrate the use of L-DPN in the fabrication of supports for protein crystallization, which consist of arrays of chemically functionalized lipid patches. DPN was performed on a DPN 5000 system (Nanoink, USA) with cantilever arrays consisting of 12 tips with either 66 or 100 μm pitch, depending on the experiment (M-Probes, Nanoink, USA).The tips were coated with lipid mixtures consisting of DOPC with either 5 mol % addition of biotin-DOPE or 1,2-dioleoyl-*sn*-glycero-3-phospho-ethanolamine-*N*-(lissamine rhodamine B sulfonyl) (rhodamine-DOPE), respectively (all lipids from Avanti Polar Lipids, USA). Generally, the first tip was coated with the fluorescent mixture containing rhodamine-DOPE, the second tip was left uncoated, and the other 10 tips were coated with the

Received: November 27, 2014
Published: December 19, 2014

DOI: 10.1021/ja512141k
J. Am. Chem. Soc. 2015, 137, 154−157

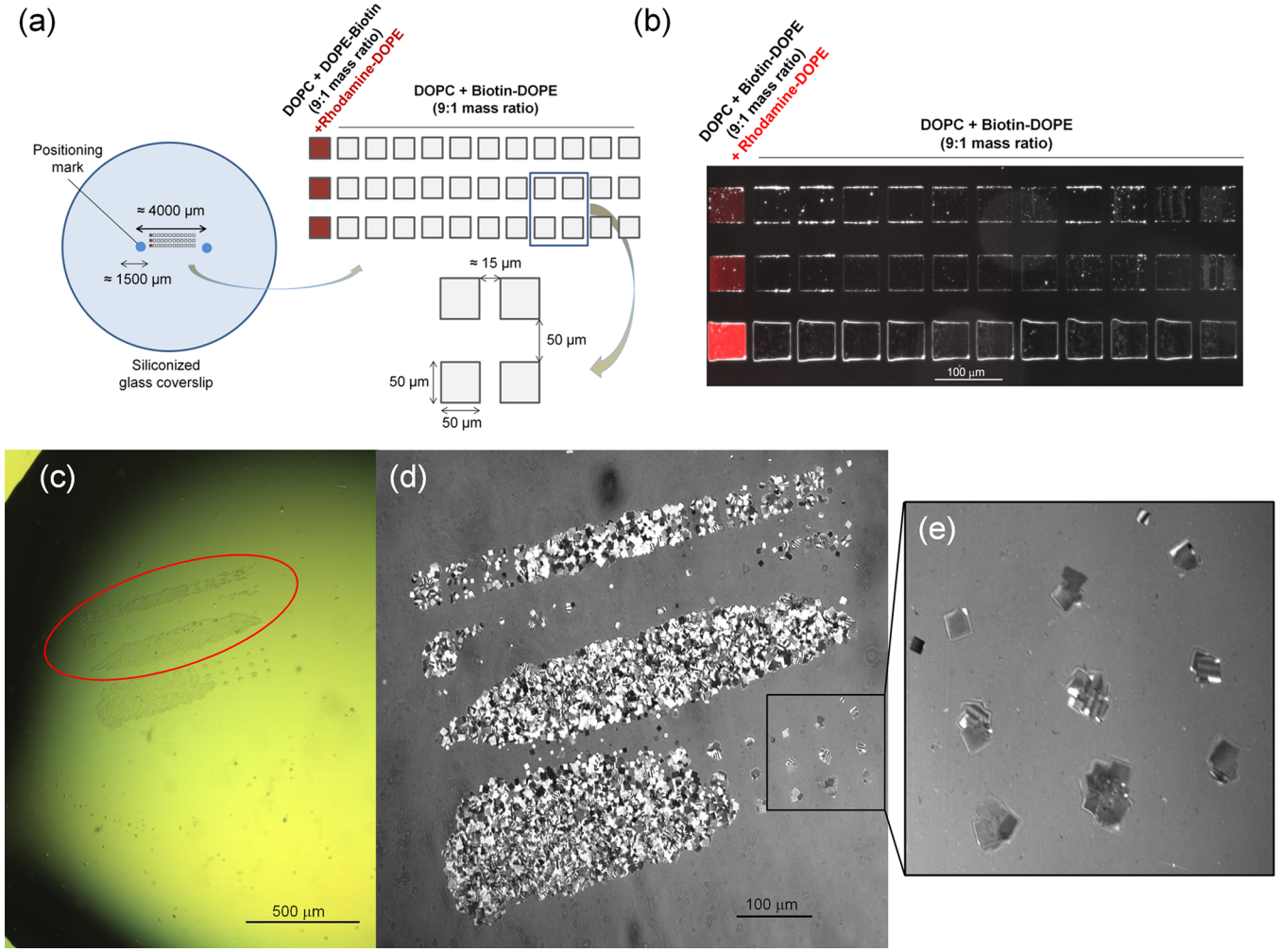

Figure 1. Vapor-diffusion crystallization on DPN-printed biotinylated lipid layers: (a) 12×3 arrays of square lipid patches were printed on siliconized glass coverslips; (b) the first column of each array was labeled with rhodamine-PE to facilitate observation by fluorescence microscopy (superposition on a dark-field microscopy image is displayed). Crystals on the lipid patches after 7 days incubation: bright-field (c) and confocal microscopy (d). Crystals were also observed in the zone below the square features (e), used to deposit lipid "dots" to remove excess ink from DPN tips.

biotin-DOPE-containing mixture. In this way, writing of the first two tips could be used as negative controls, while most tips were writing lipid patches suitable for protein adhesion and crystallization in parallel. The differently shaped features were written by hatch lines of 500 nm pitch, allowing the single lines to fuse and generate smooth membrane patches.[17] Typical line speeds for writing are between 5 and 10 μm/s with an environmental relative humidity fixed to 25−35% depending on the substrate to which the tips writing, resulting in smooth and thin membrane stacks, as desired to minimize spreading upon immersion in water.

First, the DPN-printed biotinylated lipid layers were used for streptavidin crystallization by the hanging drop method.[1] Glass surface localized DPN printing of functionalized lipid layers could have several advantages, including *in situ* protein pre-concentration and purification, the use of different lipid molecules for screening purposes, and—for difficult protein crystallization cases such as membrane proteins—the possibility of using lipid-bound or embedded 2D crystals[18] as crystallization seeds. Epitaxial growth of streptavidin crystals on lipid layers using the vapor diffusion method has been previously reported.[6a] Screening for optimal precipitant (ammonium sulfate, $AmSO_4$) and protein concentration for the formation of 3D crystals on DPN written patches gave in our hands similar results to those previously reported:[6a] 1.3 M $AmSO_4$ (32% of saturation concentration) and 10 mg/mL buffered (50 mM Tris-SO_4 pH 7.3, 100 mM NaCl) streptavidin solution. To obtain epitaxially grown streptavidin crystals, we pre-incubated for a few hours DPN-printed lipid patches on siliconized coverslips with 250 μg/mL buffered (50 mM Tris-SO_4 pH 7.3, 100 mM NaCl) streptavidin solution to form 2D crystals.[4d,6a,19]

Second, we performed hanging drop crystallization on DPN-printed patches. After 1 week of incubation at 20 °C, hundreds of streptavidin microcrystals were found on the biotinylated lipid patches (Figure 1). On one row of the lipid array, the patches were spread and fused in one single layer. This resulted in a continuous cluster of crystals, while tens of crystals formed on single square lipid patches. This experiment demonstrated that the plate-shaped microcrystals nucleated before and in a different crystal form on the lipid patches than the one found in solution, which had a prism-like shape. No crystals were found on the glass surface in the absence of biotinylated lipids.

Streptavidin was also crystallized on DPN-printed lipids using batch crystallization conditions.[1] Batch crystallization allows easy time-lapse microscopy imaging of protein crystal growth. In an initial experiment, batch crystallization was performed on

DOI: 10.1021/ja512141k
J. Am. Chem. Soc. 2015, 137, 154−157

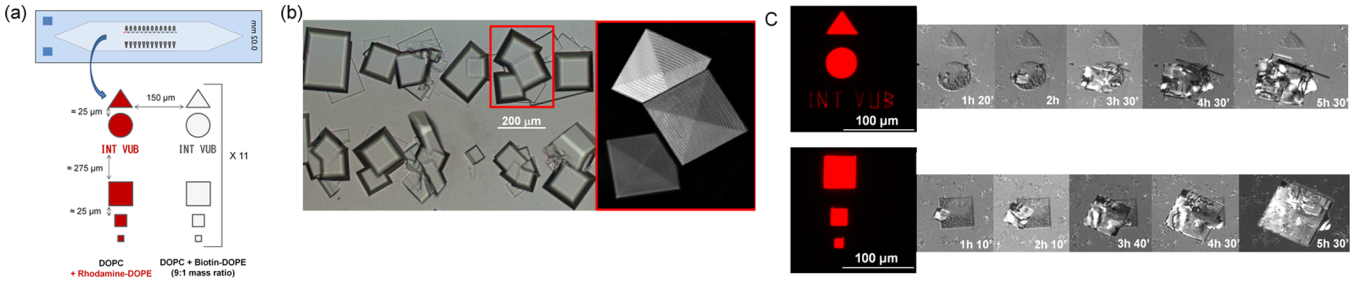

Figure 2. Batch crystallization of streptavidin on biotinylated lipid layers. An array of lipid patterns (width: 50 μm for all patches, 25 and 13 μm for smaller squares) was printed on the surface of a quartz cuvette (a). Crystals on the patterns after 5 days: bright-field microscopy (b), and LCM-DIM (red rectangle), showing the 3D spiral growth mode. Time-lapse LCM-DIM imaging (c) (fluorescence images of rhodamine-labeled lipid layers on the left; indicated are incubation times after the crystallization setup).

common coverslips in 40 μL chambers (Secure-Seal hybridization chambers, Sigma-Aldrich). The biotinylated lipid patches were pre-incubated with a 250 μg/mL streptavidin concentration to obtain surface nuclei. We obtained the best results again with 1.3 M $AmSO_4$ but more than double the protein concentration (25 mg/mL) as final conditions in the crystallization chambers (Figure S1). Again, crystals on the L-DPN-printed surfaces were the first to appear after overnight incubation at 20 °C, while other crystals nucleated in the bulk solution in 1 day time.

The same conditions were applied for streptavidin crystallization on lipid patches in quartz cuvettes, which allowed high-resolution time-lapse laser confocal microscopy (LCM) combined with differential interference contrast (DIC) microscopy[20] (Figure 2). The shape and dimensions of the biotinylated lipid patterns were varied during the DPN printing to investigate the possible effects of these variables on the subsequent crystallization process. The differences in the lipid layer shapes did not seem to significantly affect the crystal growth behavior, although the pitch of the array was not large enough to perfectly determine the final influence of each shape on the number and the dimensions of the crystals. Independently of the shape of the patches, after a few hours one or more growing crystals could be observed on the biotinylated lipid patches, expanding beyond the limits of the lipid features. The printed lipids layers were very stable during crystallization since the lipid patches showed minimal spreading and deformation, even after a few days (Figure S2 and Video S1). Furthermore, lipid layers without biotinyl-DOPE were devoid of protein crystals, confirming the specificity of biotinylated patterns in promoting crystallization on the surface, even at relatively high protein concentrations.

Finally, we demonstrate that L-DPN-assisted protein crystallization on lipid patches can be easily integrated into a microfluidic chip. Microfluidics offers several advantages for protein crystallization such as reduced sample size and easy preparation, fine control over transport phenomena on the microscale, and ease of scalability.[21] Furthermore, X-ray-transparent microfluidic devices that eliminate manual crystal handling have been recently developed.[22] Since in our approach the crystals are attached to a substrate, the crystallization growth conditions could be controlled dynamically, which allows controlling kinetically protein crystal nucleation and growth. By controlling the supersaturation in the channel, 2D nucleation can be decoupled from the growth step. In this way, growth toward large and high-quality crystals can be optimized, as was previously demonstrated in free interface diffusion microfluidic reaction chambers[23] and microfluidic drop screenings.[24] Localized protein crystallization could also facilitate the fabrication of microfluidic–enzymatic biosensors[25] (i.e., enzyme crystal-based biosensors[26]), which could be integrated in lab-on-a-chip systems.[27]

In the microfluidic setup, the arrays were printed with the same shapes as the ones designed for the batch crystallization experiments in the quartz cuvette, but smaller dimensions and larger distances between the lipid features were adopted (Figure S3), which allowed evaluating accurately the effect of the size and shape of the patches on the crystal morphology. 2D/3D crystallization conditions were as used in the batch experiments. Arrays of crystals were obtained (Figure 3 and Video S2).

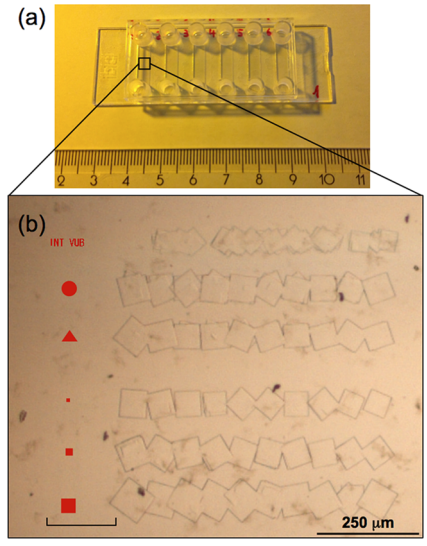

Figure 3. Streptavidin crystallization in a microfluidic sticky-slide $VI^{0.4}$ chip (Ibidi) (a) in which arrays of biotinylated lipid patches were printed. Negative controls: a nonbiotinylated, fluorophore-labeled lipid (red symbols) column and a non-inked print zone (bracket). Overnight incubation with 25 mg/mL streptavidin–$AmSO_4$ solution (b) (see also Figure S3 and Video S2).

Interestingly, we observed that the dimension of the square features influenced the average dimensions of the crystals (the bigger the features, the larger the streptavidin plates), while in the case of the "INT-VUB" patterns, merged bundles of smaller crystals were formed. It seems that larger lipid layers may generate a higher number of crystallization nuclei, which merge into a single 2D crystal and generate a larger epitaxially grown crystal. On the other hand, a high density of small features (the lipid "letters") may act as isolated crystallization nuclei, resulting in a higher number of densely packed smaller 3D crystals. These results indicate that DPN-assisted crystallization, among the

DOI: 10.1021/ja512141k
J. Am. Chem. Soc. 2015, 137, 154–157

other advantages for crystallization, would allow tuning the number and dimensions of the protein crystals. The lower limit dimensions for the biotinylated lipid layers were 2.5 × 2.5 μm in the case of the smaller square patterns, and 0.5 μm width in the case of the letter patterns. However, it is likely that even smaller patterns may promote crystal growth.

■ ASSOCIATED CONTENT

Supporting Information

Figures S1−S3 and Videos S1 and S2. This material is available free of charge via the Internet at http://pubs.acs.org.

■ AUTHOR INFORMATION

Corresponding Authors

michael.hirtz@kit.edu
ronnie.willaert@vub.ac.be

Notes

The authors declare no competing financial interest.

■ ACKNOWLEDGMENTS

The Karlsruhe Nano Micro Facility (KNMF, www.knmf.kit.edu), a Helmholtz Research Infrastructure at Karlsruhe Institute of Technology (KIT, www.kit.edu), the Belgian Federal Science Policy Office, the European Space Agency PRODEX program, the Agency for Innovation by Science and Technology (IWT, Belgium), and the Vrije Universiteit Brussel supported this work.

■ REFERENCES

(1) McPherson, A.; Gavira, J. A. *Acta Crystallogr. F: Struct. Biol. Commun.* **2014**, *70*, 2.

(2) (a) Caffrey, M. *J. Struct. Biol.* **2003**, *142*, 108. (b) Chayen, N. E. *Curr. Opin. Struct. Biol.* **2004**, *14*, 577. (c) Seddon, A. M.; Curnow, P.; Booth, P. J. *Biochim. Biophys. Acta* **2004**, *1666*, 105. (d) Wiener, M. C. *Methods* **2004**, *34*, 364. (e) DeLucas, L. J.; Hamrick, D.; Cosenza, L.; Nagy, L.; McCombs, D.; Bray, T.; Chait, A.; Stoops, B.; Belgovskiy, A.; William Wilson, W.; Parham, M.; Chernov, N. *Prog. Biophys. Mol. Biol.* **2005**, *88*, 285. (f) Chayen, N. E.; Saridakis, E. *Nat. Methods* **2008**, *5*, 147.

(3) (a) Ubarretxena-Belandia, I.; Stokes, D. L. *Adv. Protein Chem. Struct. Biol.* **2010**, *81*, 33. (b) Wisedchaisri, G.; Reichow, S. L.; Gonen, T. *Structure* **2011**, *19*, 1381. (c) Collinson, I.; Vonck, J.; Hizlan, D. *Methods Mol. Biol.* **2013**, *1033*, 47. (d) Fujiyoshi, Y. *Methods Mol. Biol.* **2013**, *955*, 551. (e) Goldie, K. N.; Abeyrathne, P.; Kebbel, F.; Chami, M.; Ringler, P.; Stahlberg, H. *Methods Mol. Biol.* **2014**, *1117*, 325.

(4) (a) Blankenburg, R.; Meller, P.; Ringsdorf, H.; Salesse, C. *Biochemistry* **1989**, *28*, 8214. (b) Darst, S. A.; Ahlers, M.; Meller, P. H.; Kubalek, E. W.; Blankenburg, R.; Ribi, H. O.; Ringsdorf, H.; Kornberg, R. D. *Biophys. J.* **1991**, *59*, 387. (c) Darst, S. A.; Edwards, A. M. *Curr. Opin. Struct. Biol.* **1995**, *5*, 640. (d) Reviakine, I.; Brisson, A. *Langmuir* **2001**, *17*, 8293. (e) Edwards, T. C.; Malmstadt, N.; Koppenol, S.; Hara, M.; Vogel, V.; Stayton, P. S. *Langmuir* **2002**, *18*, 7447.

(5) Ando, T.; Uchihashi, T.; Kodera, N.; Yamamoto, D.; Miyagi, A.; Taniguchi, M.; Yamashita, H. *Pflugers Arch.* **2008**, *456*, 211.

(6) (a) Edwards, A. M.; Darst, S. A.; Hemming, S. A.; Li, Y.; Kornberg, R. D. *Nat. Struct. Biol.* **1994**, *1*, 195. (b) Hemming, S. A.; Bochkarev, A.; Darst, S. A.; Kornberg, R. D.; Ala, P.; Yang, D. S.; Edwards, A. M. *J. Mol. Biol.* **1995**, *246*, 308.

(7) Kubo, T.; Hondoh, H.; Nakada, T. *Cryst. Growth Des.* **2007**, *7*, 416.

(8) (a) Piner, R. D.; Zhu, J.; Xu, F.; Hong, S.; Mirkin, C. A. *Science* **1999**, *283*, 661. (b) Ginger, D. S.; Zhang, H.; Mirkin, C. A. *Angew. Chem., Int. Ed.* **2004**, *43*, 30. (c) Wu, C. C.; Reinhoudt, D. N.; Otto, C.; Subramaniam, V.; Velders, A. H. *Small* **2011**, *7*, 989.

(9) Salaita, K.; Wang, Y.; Mirkin, C. A. *Nat. Nanotechnol.* **2007**, *2*, 145.

(10) Lenhert, S.; Sun, P.; Wang, Y.; Fuchs, H.; Mirkin, C. A. *Small* **2007**, *3*, 71.

(11) Sekula, S.; Fuchs, J.; Weg-Remers, S.; Nagel, P.; Schuppler, S.; Fragala, J.; Theilacker, N.; Franzreb, M.; Wingren, C.; Ellmark, P.; Borrebaeck, C. A.; Mirkin, C. A.; Fuchs, H.; Lenhert, S. *Small* **2008**, *4*, 1785.

(12) Hirtz, M.; Oikonomou, A.; Georgiou, T.; Fuchs, H.; Vijayaraghavan, A. *Nat. Commun.* **2013**, *4*, 2591.

(13) (a) Sekula-Neuner, S.; Maier, J.; Oppong, E.; Cato, A. C.; Hirtz, M.; Fuchs, H. *Small* **2012**, *8*, 585. (b) Oppong, E.; Hedde, P. N.; Sekula-Neuner, S.; Yang, L.; Brinkmann, F.; Dörlich, R. M.; Hirtz, M.; Fuchs, H.; Nienhaus, G. U.; Cato, A. C. *Small* **2014**, *10*, 1991.

(14) (a) Bog, U.; Laue, T.; Grossmann, T.; Beck, T.; Wienhold, T.; Richter, B.; Hirtz, M.; Fuchs, H.; Kalt, H.; Mappes, T. *Lab Chip* **2013**, *13*, 2701. (b) Rath, P.; Hirtz, M.; Lewes-Malandrakis, G.; Brink, D.; Nebel, C.; Pernice, W. H. P. *Adv. Opt. Mater.* **2014**, DOI: 10.1002/adom.201400434..

(15) Zhang, X.; Weeks, B. L. *J. Am. Chem. Soc.* **2014**, *136*, 1253.

(16) Liu, X.; Zhang, Y.; Goswami, D. K.; Okasinski, J. S.; Salaita, K.; Sun, P.; Bedzyk, M. J.; Mirkin, C. A. *Science* **2005**, *307*, 1763.

(17) Hirtz, M.; Corso, R.; Sekula-Neuner, S.; Fuchs, H. *Langmuir* **2011**, *27*, 11605.

(18) (a) Levy, D.; Chami, M.; Rigaud, J. L. *FEBS Lett.* **2001**, *504*, 187. (b) Dezi, M.; Fribourg, P. F.; Cicco, A. D.; Jault, J. M.; Chami, M.; Lévy, D. *J. Struct. Biol.* **2011**, *174*, 307.

(19) Scheuring, S.; Muller, D. J.; Ringler, P.; Heymann, J. B.; Engel, A. *J. Microsc.* **1999**, *193*, 28.

(20) Sleutel, M.; Maes, D.; Wyns, L.; Willaert, R. *Cryst. Growth Des.* **2008**, *8*, 4409.

(21) (a) Hansen, C.; Quake, S. R. *Curr. Opin. Struct. Biol.* **2003**, *13*, 538. (b) Stone, H. A.; Stroock, A. D.; Ajdari, A. *Annu. Rev. Fluid Mech.* **2004**, *36*, 381.

(22) (a) Gerdts, C. J.; Elliott, M.; Lovell, S.; Mixon, M. B.; Napuli, A. J.; Staker, B. L.; Nollert, P.; Stewart, L. *Acta Crystallogr. D: Biol. Crystallogr.* **2008**, *64*, 1116. (b) Ng, J. D.; Clark, P. J.; Stevens, R. C.; Kuhn, P. *Acta Crystallogr. D: Biol. Crystallogr.* **2008**, *64*, 189. (c) Dhouib, K.; Khan Malek, C.; Pfleging, W.; Gauthier-Manuel, B.; Duffait, R.; Thuillier, G.; Ferrigno, R.; Jacquamet, L.; Ohana, J.; Ferrer, J. L.; Théobald-Dietrich, A.; Giegé, R.; Lorber, B.; Sauter, C. *Lab Chip* **2009**, *9*, 1412. (d) Perry, S. L.; Guha, S.; Pawate, A. S.; Bhaskarla, A.; Agarwal, V.; Nair, S. K.; Kenis, P. J. *Lab Chip* **2013**, *13*, 3183. (e) Khvostichenko, D. S.; Schieferstein, J. M.; Pawate, A. S.; Laible, P. D.; Kenis, P. J. *Cryst. Growth Des.* **2014**, *14*, 4886.

(23) Hansen, C. L.; Classen, S.; Berger, J. M.; Quake, S. R. *J. Am. Chem. Soc.* **2006**, *128*, 3142.

(24) Zheng, B.; Tice, J. D.; Roach, L. S.; Ismagilov, R. F. *Angew. Chem., Int. Ed.* **2004**, *43*, 2508.

(25) (a) Heo, J.; Crooks, R. M. *Anal. Chem.* **2005**, *77*, 6843. (b) Lu, D.; Shao, G.; Du, D.; Wang, J.; Wang, L.; Wang, W.; Lin, Y. *Lab Chip* **2011**, *11*, 381. (c) Medina-Plaza, C.; de Saja, J. A.; Rodriguez-Mendez, M. L. *Biosens. Bioelectron.* **2014**, *57*, 276. (d) Bragazzi, N. L.; Pechkova, E.; Scudieri, D.; Terencio, T. B.; Adami, M.; Nicolini, C. *Crit. Rev. Eukaryot. Gene Expr.* **2012**, *22*, 197.

(26) (a) Luiz de Mattos, I.; Lukachova, L. V.; Gorton, L.; Laurell, T.; Karyakin, A. A. *Talanta* **2001**, *54*, 963. (b) Roy, J. J.; Abraham, T. E. *Chem. Rev.* **2004**, *104*, 3705. (c) Roy, J. J.; Abraham, T. E.; Abhijith, K. S.; Kumar, P. V.; Thakur, M. S. *Biosens. Bioelectron.* **2005**, *21*, 206. (d) Laothanachareon, T.; Champreda, V.; Sritongkham, P.; Somasundrum, M.; Surareungchai, W. *World J. Microbiol. Biotechnol.* **2008**, *24*, 3049.

(27) (a) Mark, D.; Haeberle, S.; Roth, G.; von Stetten, F.; Zengerle, R. *Chem. Soc. Rev.* **2010**, *39*, 1153. (b) Kumar, S.; Kumar, S.; Ali, M. A.; Anand, P.; Agrawal, V. V.; John, R.; Maji, S.; Malhotra, B. D. *Biotechnol. J.* **2013**, *8*, 1267.

DOI: 10.1021/ja512141k
J. Am. Chem. Soc. 2015, 137, 154−157